Autonomous Raman amplifiers in multi-band software-defined optical transport networks

*To be published in Journal of Optical Communications and Networking:*

**Title:** Autonomous Raman Amplifiers in Multi-Band Software-Defined Optical Transport Networks

**Authors:** Giacomo Borraccini,Stefano Straullu,Andrea D'Amico,Antonino Nespola,Stefano Piciaccia,Alberto Tanzi,Gabriele Galimberti,Vittorio Curri

**Accepted:** 12 May 21

**Posted** 12 May 21

**DOI:** https://doi.org/10.1364/JOCN.424025

# Autonomous Raman Amplifiers in Multi-Band Software-Defined Optical Transport Networks

GIACOMO BORRACCINI[1*], STEFANO STRAULLU[2], ANDREA D'AMICO[1], ANTONINO NESPOLA[2], STEFANO PICIACCIA[3], ALBERTO TANZI[3], GABRIELE GALIMBERTI[3], AND VITTORIO CURRI[1]

[1] DET, Politecnico di Torino, corso Duca degli Abruzzi, 24, Torino (TO), 10129, Italy
[2] LINKS Foundation, via Pier Carlo Boggio, 61, Torino (TO), 10138, Italy
[3] Cisco Photonics, via S. M. Molgora, 48/C, Vimercate (MI), 20871, Italy
[*] Corresponding author: giacomo.borraccini@polito.it

Compiled May 11, 2021

**A controller architecture for managing multi-band Raman amplification within software-defined optical transport networks (SD-OTN)s is presented. In the perspective of optical fiber network softwarization and disaggregation, this work provides an operative description of a system capable to autonomously handle Raman amplification on a single fiber span, achieving the working point requested by the control plane in terms of mean gain and tilt. The developed architecture is composed by two software modules: the Raman Design Unit (RDU) and the Raman Controller Unit (RCU). Firstly, the RDU defines the nominal optimal working point designing the power level configuration of the Raman card pumps according to the required amplification constraints without considering any channel spectral load. Then, thanks to the telemetry feedback, the RCU performs a tracking operation of the mean gain towards the target one, linearizing the problem at the nominal optimal working point. The fiber physical parameters needed by the controller for a correct operation of the system are extracted through a conceived probing procedure. The proposal shows a high degree of adaptability of the such defined Raman amplifier to the particular in-field scenario in which it is deployed, also counteracting spectral load modifications. The behavior of the described system is validated by means of an experimental session, confirming the effectiveness of the controller architecture design and the high accuracy achieved in terms of performance.** 

http://dx.doi.org/10.1364/ao.XX.XXXXXX

## 1. INTRODUCTION

Driven by the expected sharp increase of global Internet users and by the fulfilment of 5G, optical communications are covering a key role among the various technological areas in improving services for both private and industrial scopes. In the last decades, in addition to the strengthening of the actual infrastructures and the creation of new solutions, the focus of research – and also of the market – has pointed towards systems that deeply exploit features of the already installed resources, taking full advantage from them. Going into detail, within the field of optical fiber networks, design of amplification sites and their management within a software-defined network (SDN) context turn out to be fundamental factors in the achievement of high performance systems with larger capabilities. For this purpose, a consolidated amplification technology in optical transport networks (OTN)s renowned for its feature of producing a lower equivalent noise figure with respect to standard systems based on Erbium-doped fiber amplified (EDFA) is Raman amplification (RA) [1, 2]. Thanks to its characteristic of keeping low the amplified spontaneous emission (ASE) noise generation [3, 4], the use of Raman amplifiers is sensibly favoured in the realization of long-haul optical communication systems [5, 6]. Furthermore, given the broad-band impact, this kind of amplification allows to manage very dense wavelength division multiplexing (DWDM) spectra, enabling multi-band transmissions [7, 8]. In terms of maximum reach and noise degradation, a remarkable trade-off is obtained adopting Erbium-doped/Raman amplifiers (EDRA)s, which combine high performance with a relative low noise generation thanks to the exploitation of both the amplification technologies [9].

Considering the field of long-haul multi-band transmissions, the increment of computational power available on-board of recent controller devices have allowed the softwarization and the disaggregation of the optical network, giving birth to the SDN [10] and improving the service management by means of the implementation of more sophisticated models and optimization algorithms. At the same time, the physical layer characterization has become a fundamental step of the probing

procedure in order to adequately feed and effectively exploit such calculation tools. As a consequence, these factors have kicked off the birth of cognitive optical networks [11], in which the network infrastructure becomes an entity aware of the context where it is immersed and able to take decisions, to learn and to optimize features. Referring specifically to the physical layer, in addition to the difficulty of acquiring a sufficient amount of information from the optical domain, in-field operations of a generic network are affected by various scenario modifications, such as fiber cuts, component aging and temperature. These variables deeply notch the system performance, especially in case of multi-band DWDM, where Raman cross-talk becomes a dominant effect and small variations of channel power levels can sensibly move the working point far from the expected one [12].

In order to achieve effective designs of cognitive optical networks, these infrastructures must be composed by software modules that confer dynamism and flexibility to the installed equipment, basing their action on a robust probing procedure and exploiting the feedback of telemetry devices. Artificial intelligence and machine-learning (ML) techniques seem to offer an effective solution, even if the achievement of a suitable in-field data-set is not given for free in terms of time. Also in this case, scenario modifications can easily alter the conditions captured during data-set measurements, even creating significant mismatches between the physical model absorbed by the single controller and the real one.

From an historical point of view, in order to enable the use of Raman amplification in optical communications, the first approach was to mathematically address the optimization problem related to the achievement of amplification constraints, ranging between extremely different methodologies [13–17]. Thanks to the multiple benefits provided, Raman amplifiers were considered right away in innovative optical network designs that massively exploit the fiber link capacity, such as SDNs [10, 18, 19]. In parallel, various research activities have investigated network solutions that include the feature of cognition at any abstraction level of the system, pushing towards the concept of aware and autonomous optical networks [11, 20, 21]. Raman amplification has been recently addressed even through the implementation of ML techniques, reaching high levels of efficiency and accuracy in terms of performance [22–24] if a large dataset can be collected.

This work provides an operative description of a software controller capable to autonomously handle Raman amplification on a single fiber span in a context of software-defined optical transport network (SD-OTN), achieving the working point requested by the control plane in terms of mean gain and tilt. The authors have already outlined and experimentally tested the capability of locally managing Raman amplification of the proposed controller architecture exploring different scenarios and specific features. In particular, [25] focuses on the softwarization of the Raman amplifier and on the mathematical formalization of the optimization framework that determines the configuration of Raman pump power levels given both a physical layer description and the target values of mean gain and tilt. [26] is an experimental proof of the flexibility and of the adaptation capability of the Raman amplifier architecture, showing its usage both in single- and multi-band scenarios with the possibility to accurately control the DWDM spectrum tilt. In [27], a complete probing procedure that enables the automation of the Raman amplifier relying on the optical time domain reflectometer (OTDR) and optical channel monitors (OCM)s is described and experimentally proved. [28] provides the application of this Raman amplifier controller within a C-band scenario using minimal in-field telemetry support, as standard integrated photodiodes.

The purpose of this work is twofold. Firstly, it operates a comprehensive synthesis of the previous research activities, returning a complete and accurate description of each part of the developed software framework. Furthermore, the use of this architecture in real implementations is explained highlighting each procedural step starting from the hardware installation to the network operative phase. Secondly, the novelty relies on the proposal of a simplified probing procedure for the physical layer characterization both in single- or multi-band scenarios and on the introduction of efficient analytical linearization techniques that maximize adaptability and flexibility, facing up issues related to modifications of the spectral load or of the physical layer and providing a valuable solution for real-time applications. In this study, the ASE noise generated by the Raman amplification is not considered, as this impairment is not an optimization variable of the investigated scenario.

The paper is divided into five sections. Sec. 2 describes the network scenario assumed in order to operate the softwarization of the Raman amplifier. Sec. 3 shows the structure of the Raman amplifier controller software that has been developed and a general overview of its behaviour, highlighting the characteristics, the role of each module and the various relationship between the players operating in the scenario. Sec. 4 reports the detailed probing procedure used to abstract the physical layer information needed by the controller. Sec. 5 provides the complete mathematical formulation of each part of the control software framework. In Sec. 6, the behavior of the described system is analyzed and validated by means of a laboratory experimental session, showing results derived by the probing procedure and a complete set of operative steps led by the controller in order to set the optimal working point, satisfying the control plane request.

## 2. NETWORK ARCHITECTURE

We suppose to operate in a software-defined open and disaggregated optical networking scenario [29] where each network element is a white-box [30] exposing telemetry to the network controller monitors, and enabling virtualized control by open data structures, protocols and APIs [31–33]. In such a scenario, the control plane relies on a full virtualization of network element functionalities and the network control is fully automatized. Virtualization and full automation of optical networks require a large effort and several technical precautions regarding the drafting and the development of protocols and control

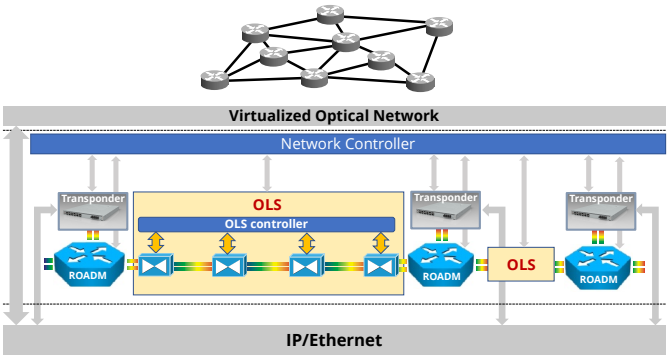


**Fig. 1.** Virtualized optical network architecture.

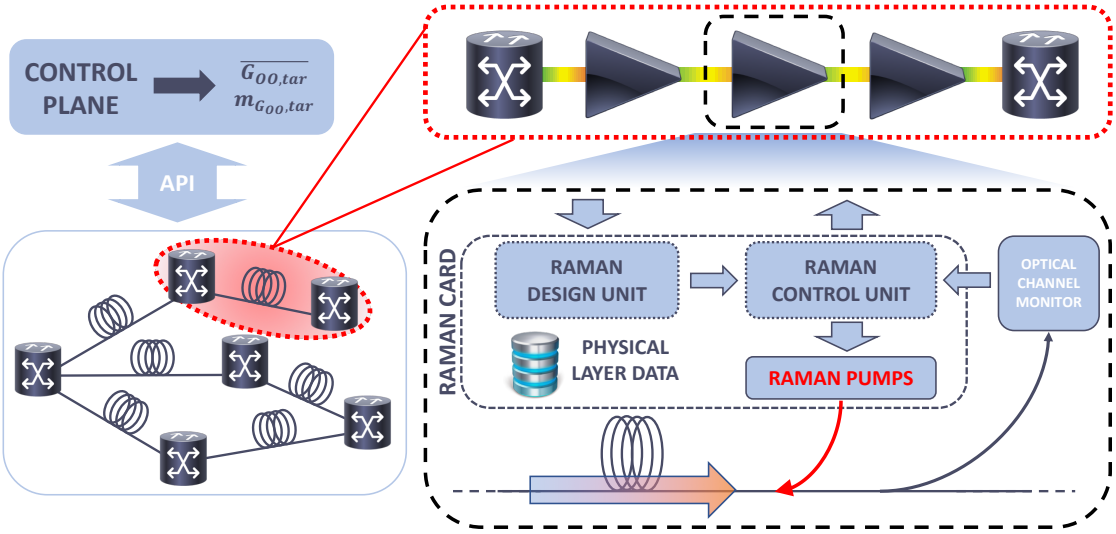


**Fig. 2.** Designed controller architecture for autonomous Raman amplifiers and network contextualization.

strategies.

A sketch of a software-defined virtualized disaggregated optical network architecture is reported in Fig. 1. At any level of abstraction, the goal of the virtualization process is to handle network elements as single and independent modules able to autonomously execute specific tasks. This management of optical networks implies the increase of local complexity in the system, conveying control protocol information and reducing execution time. The behaviour of the overall frame is harmonized through the work of high-level-abstraction controllers, which manage the optical network relying on the interaction with the other units. Regarding physical layer cognition, the basis on which this concept of optical network architecture rests is the extraction of information by the set of software modules that work at physical layer on the optical domain. In fact, probing phase becomes a necessary step within the work-chain of network elements' automation in order to robustly determine the wanted system working point, avoiding databases which contain physical layer information estimated a priori. The use of information related to the optical domain without in-field probing allows to achieve satisfying levels of accuracy only in case of deep knowledge of the installed hardware and if the scenario does not undergo substantial modifications (e.g., fiber cut&splicing). Therefore, the only procedure enabling a reliable data structure for physical layer is to read data from monitors by telemetry.

## 3. RAMAN AMPLIFIER CONTROLLER ARCHITECTURE

A proof-of-concept for the conceived Raman amplifier controller within a SDN is presented, providing a full description of the control process with the related information exchanged between monitoring devices and software modules. In general, the implementation can be realized using the most appropriate protocols for the specific scenario. The architecture of the designed autonomous Raman amplifier is illustrated in Fig. 2, starting from an optical network context and zooming towards a single amplification site. The embedded system is composed by two software modules: the Raman Design Unit (RDU) and the Raman Controller Unit (RCU). Firstly, the RDU defines the optimal working point designing the power level configuration of the Raman card pumps according to the requested amplification mask without considering any channel spectral load. Then, thanks to the telemetry feedback, the RCU performs a tracking operation of the mean gain towards the target one, linearizing the problem around the optimal working point.

Focusing on the behavioral aspect of the proposed Raman controller architecture, let us consider the entire process that bring an optical line system to work within an optical network. After the installation of an optical link within the network, each Raman amplifier is calibrated by means of a probing procedure, conceived to acquire the physical layer knowledge needed by the RDU for the optimization. At this point, Raman amplifiers are ready to use and the work-flow starts with the definition of the amplification constraints in terms of mean gain and tilt for each amplification site by the control plane. Locally, Raman controllers receive the description of the respective gain-mask target and each RDU proceeds with the definition of the Raman pump power configuration that matches amplification constraints. This optimization phase is performed regardless of the channel spectral load, considering only inter-pump effects. In addition to the optimal Raman pump power configuration, the RDU also computes in advance the power gradients for each pump with respect to the gain variation, which are parameters that will be used by the RCU in order to perform the adjustment of the mean gain profile. This step is done internally by the optimization framework before the start of real in-line operations. Subsequently, the RCU is in charge of setting Raman pump power levels according to the computed configuration. Thanks to a linearization algorithm based on the gradients' evaluation performed by the RDU, the RCU controls the Raman pumps varying their power levels in order to achieve the mean gain, exploiting telemetry data provided by OCMs. The latter are located at the receiver side of the considered fiber span in order to monitor the status of propagating spectrum resolute in frequency after the amplification.

The proposed controller architecture implies several advantages regarding the adaptability to the physical layer features of the scenario in which the system is inserted and the flexibility with respect to spectral load variations. In particular, the anatomy of the controller combined with the currently only mentioned probing procedure allow to easily manage cases of fiber cuts or components' aging, which are probable issues re-

lated to the scenario modifications. The conceived framework is able to support both multi-band and single-band transmission following to the necessities of the network. The focus of the optimization process is to define a Raman pump power level configuration that matches the target given a set of Raman pumps at specific frequencies. The implementation can be extended in order to include the design of the optimal frequencies of the Raman pumps.

Regarding the execution for single fiber span operations, recording the optimization time for different combinations of target values, the RDU needs a computational time of the order of minutes. From an application point of view, this operation is the most time-consuming part of the control process but it is performed only once at the beginning of the operative phase of the system, and can be done simultaneously for every amplifying site as it is a local procedure. So, it can be included in the line initialization procedure before the actual traffic deployment. When the optimal Raman configuration is set, the RCU performs simple analytical computations in order to adjust the mean gain towards the gain target with real-time response. Thus, the RCU may exploit edge-computing available on network elements, so guaranteeing a quick response and consequent adaptation to possible variations in physically layer.

The developed framework is embedded for the management of pure Raman amplification. In future investigations, the definition of a more general EDRA controller architecture can be addressed implementing a software wrapper that includes the single controllers for the two types of amplification. In the next sections, a more detailed view of the probing procedure and of the software module contents is provided, even reporting information and clarifications about the choice of the adopted strategies and protocols.

## 4. PHYSICAL LAYER PROBING

As premises, to achieve reliable results from the probing procedure, Raman pumps undergo a preliminary calibration step in which each one has to be tuned in order to inject through the fiber the desired amount of optical power. The presence along the link of the optical devices with non-flat frequency response must be singularly taken into account and adequately characterized.

The whole controller framework is based on the knowledge of the following physical parameters of the fiber link:

- the fiber span length $L_S$;
- the lumped losses along the fiber span $l_c(z)$;
- the Raman efficiency of the fiber $C_R(\Delta f)$;
- the loss coefficient function $\alpha(f)$;

In order to make the probing procedure applicable to the largest possible number of contexts but keeping limited the complexity, some simplifications about the acquisition are operated without losing final result accuracy. In condition of uniform fiber, it is possible to assert that, known the kind of fiber, the Raman coupling due to the specific fiber link does not significantly change [1, 34], and so the Raman efficiency profile $C_R(\Delta f)$ can be fixed in advance without making a considerable error.

In order to fill the lack of physical layer knowledge, some artificial parameters are introduced and extracted during the probing procedure. They are called *correction parameters* and are offset values that allow the optimization tool to adequately

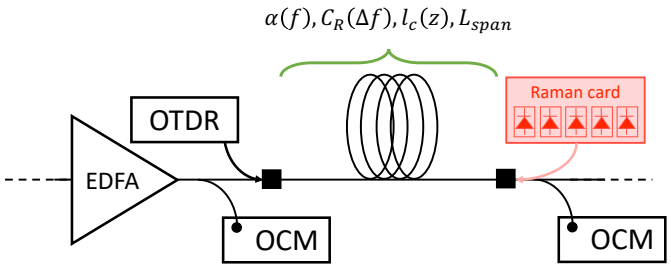


**Fig. 3.** Sketch of the assumed single fiber span scenario with the supplied telemetry devices.

recenter the emulated gain-mask both in terms of mean gain $\overline{G_{OO,cor}}$ and gain profile slope $m_{G_{OO},cor}$.

The assumed scenario for a single fiber span is depicted in Fig. 3. The probing procedure is articulated in four steps in which the extraction of the needed physical layer information is performed. In detail, the proposed protocol aims to acquire:

- span length $L_S$ and lumped losses $l_c(z)$;
- loss coefficients for channel frequencies $\alpha(f_{ch})$;
- loss coefficients for pump frequencies $\alpha(f_p)$;
- correction parameters $\overline{G_{OO,cor}}$, $m_{G_{OO},cor}$.

### A. OTDR Analysis

The first step consists in a fiber span analysis using the OTDR. The aim is to estimate the span length $L_S$ and to identify position and entity of lumped losses $l_c(z)$ located along the fiber link due to possible splices, connectors or non-idealities.

### B. Complete WDM Spectrum Propagation

During the following step, an analytical computation of the loss coefficient function for channel frequencies $\alpha(f_{ch})$ is performed exploiting OCM feedback. To execute calculations, the contribution due to the Raman coupling is assumed to be the theoretical Raman efficiency profile related to the known fiber type. The following procedure can be applied with any modern type of fiber. The theoretical Raman efficiency profile for standard single-mode fiber (SSMF) is shown in Fig. 4. During this phase, Raman pumps remain turned off.

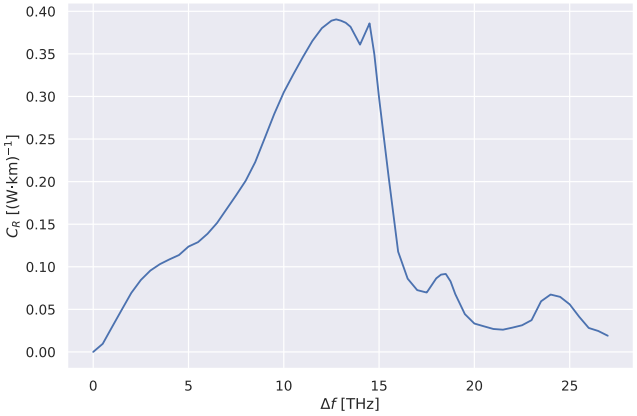


**Fig. 4.** Theoretical Raman efficiency profile for standard single-mode fiber (SSMF).

The procedure is articulated in the following points:

- propagation along the fiber span at low power of a full load ASE super-channel, not necessarily flat, created by means of the ASE noise generator that covers the complete frequency range;
- acquisition of the power spectra at both transmitter ($P(f_{ch},0)$) and receiver ($P(f_{ch},L_S)$) sides by OCMs;
- computation of the tilt of the received spectrum $m_P$ as the slope of its linear regression;
- estimation of the average loss coefficient $\overline{\alpha}$ by means of the following formula (logarithmic units):

$$\overline{\alpha} = \overline{\left(\frac{P(f_{ch},0) - (P(f_{ch},L_S) + \sum l_c(z))}{L_S}\right)}\,; \tag{1}$$

- emulation of the system introducing the average loss coefficient function $\overline{\alpha}$ and the theoretical Raman efficiency profile;
- computation of the power difference $\Delta P(f_{ch})$ between the effective received spectrum $P(f_{ch},L_S)$ and the emulated one $P^{EMU}(f_{ch},L_S)$:

$$\Delta P(f_{ch}) = P(f_{ch},L_S) - P^{EMU}(f_{ch},L_S)\,; \tag{2}$$

- extraction of the loss coefficient function $\alpha(f_{ch})$ through the following formula:

$$\alpha(f_{ch}) = \left(\frac{\Delta P(f_{ch})}{P(f_{ch},L_S)} + 1\right)\overline{\alpha}\,. \tag{3}$$

Eq. 3 refers to the extraction of the loss coefficient vs. frequency, starting from the difference between experimental results and emulation done with a flat loss coefficient function (Eq. 2). The frequency resolution is established a priori considering the telemetry accuracy and the adopted channel grid.

### C. Pump&Probe Measurements

To extract the loss coefficient function for Raman pump frequencies $\alpha(f_p)$, a set of pump & probe (P&P) measurements has been performed. For each Raman pump, the measurement is run exploiting as a probe the same ASE noise super-channel used in the previous step. Therefore, the on-off gain on the probe $G_{OO}$ is computed thanks to a double measurement in which the selected Raman pump is before turned off and then it is activated, measuring the total power of the probe at the receiver side by means of the OCM. The on-off gain $G_{OO}$ is intended as the overall effect that the Raman pump has on the probe. In this perspective, the Raman coupling due to the specific Raman pump on the probe is calculated as:

$$C_R(f_p) = \frac{\int_{f_p-f_{min}}^{f_p-f_{max}} C_R(\phi)d\phi}{f_{max}-f_{min}}\,, \tag{4}$$

where $C_R(\phi)$ is the assumed Raman efficiency profile integrated between the bounds of the frequency distance range determined by the selected pump and the probe total band. As the P&P measurement involves a complete spectrum at low power level and a significantly high pump launch power level $P(f_p,L_S)$, it is reasonable to assume undepleted pump [13] and so the loss coefficient function for Raman pump frequencies $\alpha(f_p)$ can be estimated using the following formula [35]:

$$L_{eff}(f_p) = \frac{ln(G_{OO})}{P(f_p,L_S)C_R(f_p)}\,, \tag{5}$$

For long fiber spans, given the expression of the effective length for the Raman pump frequency, it is reasonable to approximate the formula as follows:

$$L_{eff}(f_p) = \frac{1-e^{-\alpha(f_p)L_S}}{\alpha(f_p)} \approx \frac{1}{\alpha(f_p)}\,. \tag{6}$$

Consequently, the wanted parameters is extracted computing the inverse of the effective length $L_{eff}(f_p)$ for each Raman pump.

### D. Optimization at Maximum Gain

The last step of the probing procedure is a first Raman amplification optimization performed by the RDU at the maximum gain target $\overline{G_{OO,tar,MAX}}$ achievable by the system. After the optimization, the found optimal configuration is set and mean on-off gain $\overline{G_{OO}}$ and tilt $m_{G_{OO}}$ are extracted from telemetry. These data are compared with target values, and correction parameters are computed as follows:

$$\begin{aligned}\overline{G_{OO,cor}} &= \overline{G_{OO,tar,MAX}} - \overline{G_{OO}}\,,\\ m_{G_{OO},cor} &= m_{G_{OO},tar} + m_{G_{OO}}\,.\end{aligned} \tag{7}$$

The tilt target $m_{G_{OO},tar}$ is set to zero, being the purpose of the optimization the achievement of a flat WDM spectrum. Thanks to this step, the center of the emulated gain-mask produced by the optimization frame is restored at the correct working point, filling lack of physical layer knowledge and compensating for any uncertainty.

## 5. CONTROLLER OPERATIVE BEHAVIOR

The Raman controller is composed by two software modules that have different and specific roles within the architecture. In the following section, details about the operative behaviour of the conceived Raman controller are provided, showing structures and developed algorithms, and discussing the operation of the two modules in terms of execution time.

### A. Design Phase (RDU)

The RDU represents in fact an optimizer able to determine the power configuration of a specific set of Raman pumps that matches the amplification constraints, given a physical description of the fiber span link. The core of the RDU is a numerical solver which allows to emulate the stimulated Raman scattering (SRS) phenomenon for different pump launch power levels through a system of ordinary differential equations (ODE)s describing the power evolution $P(f_i,z)$ of channels and pumps [1].

In the case under investigation, the optimization problem can be formulated as follows:

$$\min_x f(x)$$

where $f(x)$ is the objective function. The main aim is to optimize a set of Raman pump power levels, where pump frequencies are fixed in advance. For each Raman pump, the power level ranges between zero and the maximum amount that can be delivered. In addition, the maximum total power introduced by the Raman card into the fiber cannot exceed 1 W.

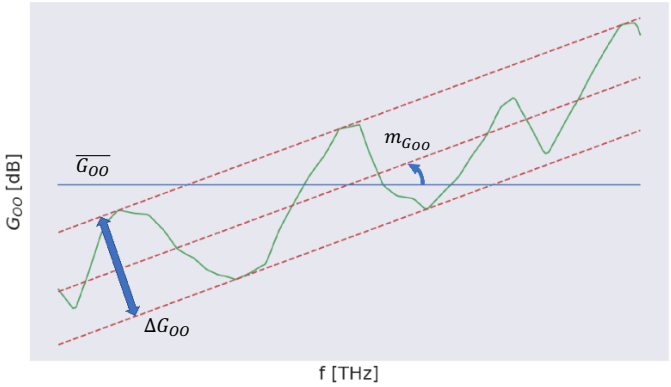


**Fig. 5.** Metrics derived from the on-off gain profile $G_{OO}$.

The problem falls in the class of constrained multi-variable nonlinear optimization problems. To cope with the latter, a deterministic minimization method called sequential least squares programming algorithm (SLSQP) has been used.

### A.1. Objective function

In the optimization procedure, only the depletion mechanism among pumps is considered while pumps vs. channels and inter-channel interactions are neglected, as the amplifiers' working point does not depend a priori on the spectral load. The on-off gain profile $G_{OO}(f_{ch})$ obtained by a single pump-channel pair is computed using the formula:

$$G_{OO}(f_{ch}) = \exp\left(\int_0^{L_S} C_R(f_{ch}, f_p) P(f_p, \zeta)\, d\zeta\right) \quad (8)$$

where $C_R(f_{ch}, f_p)$ is the Raman efficiency between the channel and the pump, $P(f_p, \zeta)$ is the pump power spatial evolution. The contribution of each pump is considered analytically identical and so the overall Raman effect on a single channel is equal to the sum of each pump contribution.

After the on-off gain profile computation, the mean value $\overline{G_{OO}}$, the angular coefficient of the linear regression $m_{G_{OO}}$ and the maximum deviation from the linear regression $\Delta G_{OO}$ are derived (Fig. 5). Thereby, the form of the objective function is:

$$f(x) = |\,\overline{G_{OO}} - \overline{G_{OO,tar}}\,| + |\,m_{G_{OO}} - m_{G_{OO},tar}\,| + \Delta G_{OO} \quad (9)$$

where $\overline{G_{OO,tar}}$ is the mean on-off gain target and $m_{G_{OO},tar}$ is the tilt target.

Generally, as the optimization procedure is performed regardless the channel spectral load present on the fiber link, the expected optimal Raman pump configuration found by the RDU undergoes some deviations from the expected result when the RCU sets the Raman card. In particular, considering the metrics of interest, the on-off gain profile produced in field can have two possible mismatches: the mean and tilt values. Actually, what is experimentally shown by this investigation is that the unique significant and appreciable drawback is related to a limited variation of the on-off gain mean value, while the slope of the linear regression is not affected. In fact, the presence of the WDM spectrum leads to a pump depletion effect which is not taken into account during the optimization process, contributing to reduce the gain-mask as a rigid shift. This issue is compensated on-line during the operation through a conceived linearization algorithm carried out by the RCU, which performs the restore of the wanted mean gain without distorting the gain profile shape. On the other hand, the input spectral load is a negligible factor for the shape of the on-off gain profile. This observation is confirmed focusing on the dynamics of the phenomena which take place along the fiber during the propagation (Fig. 6). In general, excluding phenomena related to noise generation, channels experience three main effects during their propagation along the fiber, which are the fiber attenuation, Raman cross-talk and Raman amplification. While the attenuation effect is distributed along the entire link, the impact of the Raman cross-talk and Raman amplification can be circumscribed in specific areas of the link. In particular, the WDM spectrum tilting takes place only when power levels of channels or pumps are effective: Raman cross-talk originates in the first kilometers of the fiber span due to the high power density of the WDM spectrum and Raman amplification occurs close to the span termination due to the high Raman pump powers. So, from an optimization point of view, it is possible to achieve the tilt requested by the control plane in case of enough long fiber spans in which the two Raman tilting effects can be separated.

### A.2. Gradients' Evaluation

At the end of the optimization process, before leaving the floor to the RCU, the RDU computes some parameters that are fundamental to understand how to manage Raman pump power levels in order to proceed with the linearization algorithm. For this purpose, a couple of perturbations around the optimum solution, one positive and one negative, is applied at each Raman pump in order to observe the variations of the mean gain with respect to the selected Raman pump power level. Starting from the optimum working point $P_{opt}$, the behaviour of each perturbed configuration is emulated and the relative mean gain is extracted. The perturbation applied to the selected Raman pump is a small percentage $p$% of its power level. Considering each variation of the optimum scenario, the gradient with respect to a single input parameter is computed as an incremental ratio:

$$\partial_{P^{\pm}_{opt,i}} \overline{G_{OO}} = \frac{\delta \overline{G_{OO}}}{\delta P^{\pm}(f_i, L_S)} = \frac{\overline{G_{OO,opt}} - \overline{G_{OO,opt\pm var}}}{10\log(1 \pm p\%)} \quad \left[\frac{dB}{dB}\right] \quad (10)$$

where $\overline{G_{OO,opt}}$ is the mean gain generated by the optimal Raman pump power configuration and $\overline{G_{OO,opt\pm var}}$ is the mean gain

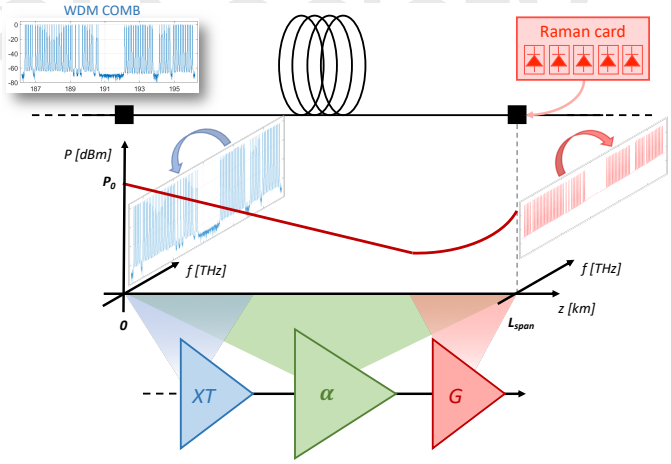


**Fig. 6.** Dynamics of the phenomena involved during the propagation along a single fiber span: fiber attenuation ($\alpha$), Raman cross-talk ($XT$) and Raman amplification ($G$).

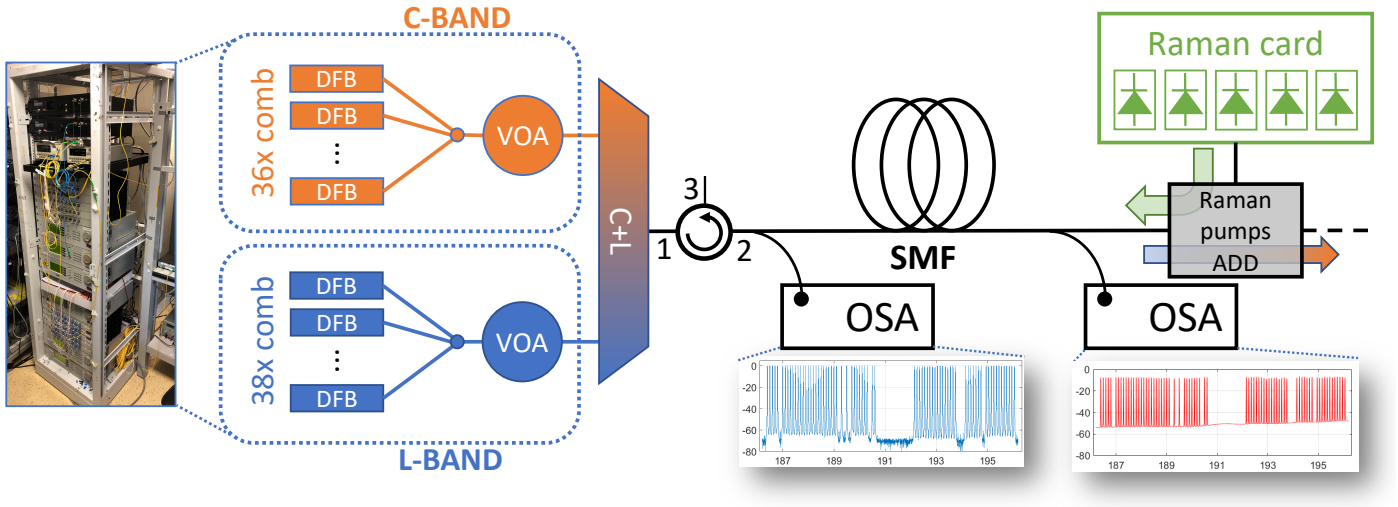


**Fig. 7.** Experimental equipment set in the photonic laboratory of LINKS Foundation, Turin.

**Algorithm 1.** Control algorithm

**procedure** RCU($P_{opt}, \partial_{P^{\pm}_{opt}} \overline{G_{OO}}$)
  $P = P_{opt}$
  $\Delta\overline{G_{OO}} = \epsilon$
  **while** $|\Delta\overline{G_{OO}}| \geq \epsilon$ **do**
    Set Raman card pumps at $P$
    Extract $\overline{G_{OO}}$ from telemetry data
    $\Delta\overline{G_{OO}} = \overline{G_{OO,tar}} - \overline{G_{OO}}$
    **if** $|\Delta\overline{G_{OO}}| \geq \epsilon$ **then**
      $P$ =LINEARIZATION($P, \partial_{P^{\pm}_{opt}} \overline{G_{OO}}, \Delta\overline{G_{OO}}$)

**Algorithm 2.** Linearization function

**function** LINEARIZATION($P, \partial_{P^{\pm}_{opt}} \overline{G_{OO}}, \Delta\overline{G_{OO}}$)
  **if** $\Delta\overline{G_{OO}} > 0$ **then**
    $S_P^{\overline{G_{OO}}} = \partial_{P^{+}_{opt}} \overline{G_{OO}}$
  **else**
    $S_P^{\overline{G_{OO}}} = \partial_{P^{-}_{opt}} \overline{G_{OO}}$
  $S_{tot} = \sum S_P^{\overline{G_{OO}}}$
  **for** each item $P_i$ in $P$ **do**
    $p_{S_i} = S_{P_i}^{\overline{G_{OO}}} / S_{tot}$
    $\Delta G_{OO,P_i} = p_{S_i} |\Delta\overline{G_{OO}}|$
    $\Delta P_i = \Delta G_{OO,P_i} / S_{P_i}^{\overline{G_{OO}}}$
    $P_{lin,i} = P_i + \Delta P_i$
  **return** $P_{lin}$

derived from the configuration with the selected Raman pump power perturbed of a percentage $\pm p\%$. The final result is a set of parameters, two for each Raman pump, which are used by the RCU to perform the adjustment of the mean gain, moving the pump power levels according to the information given by the gradients.

### B. Linearization and Control (RCU)

At this point, the RDU provides to the RCU the optimal Raman pump power configuration $P_{opt}$ and the list of the computed gradients $\partial_{P^{\pm}_{opt}} \overline{G_{OO}}$. Thanks to the telemetry feedback, the RCU performs a tracking operation of the mean gain towards the target one, linearizing the problem around the optimal working point. This procedure is performed until the gap between the actual mean gain and the target one $\Delta\overline{G_{OO}}$ is below a fixed threshold $\epsilon$ (Alg. 1).

At each iteration, the linearization procedure is applied to the current Raman pump configuration $P$ (Alg. 2). The key idea is to proportionally divide the mean gain gap with respect to the target one $\Delta\overline{G_{OO}}$ according to the gradient entity of each Raman pump around the optimum working point $\partial_{P^{\pm}_{opt}} \overline{G_{OO}}$. $S_P^{\overline{G_{OO}}}$ represents the list of sensitivities used for linearizing the working point, which is selected between $\partial_{P^{+}_{opt}} \overline{G_{OO}}$ and $\partial_{P^{-}_{opt}} \overline{G_{OO}}$ related to the sign of $\Delta\overline{G_{OO}}$. All the values within $S_P^{\overline{G_{OO}}}$ have the same sign by construction. $S_{tot}$ is defined as the sum of all the values that appear in $S_P^{\overline{G_{OO}}}$. This process has been designed in order to rapidly operate adjustments of the mean gain without distorting the on-off gain profile shape. Being a linearization procedure, it is effective around the computed optimum for small gain ranges up to 1 dB, preserving the on-off gain profile shape. During the undertaken experimental campaign, deviations above this threshold have not been recorded.

## 6. EXPERIMENTAL RESULTS

In order to verify the behavior of the entire controller architecture and to validate the effectiveness of the probing procedure, an experimental campaign has been fulfilled. In this section, the experimental equipment is firstly described. Then, the probing phase results are shown and commented in order to remark the meaning of the performed steps. Finally, the experimental results proving the operative behavior of the conceived Raman amplifier are reported.

### A. Experimental Setup

The experimental equipment is sketched in Fig. 7. A comb of distributed feedback (DFB) lasers composes the input WDM spectrum. By using a continuous-wave (CW) comb we do not lose in generality, as Raman gain is not sensible to the signal modulation but only to the average power level. In particular, two input WDM spectra are created in L-band (38 channels) and

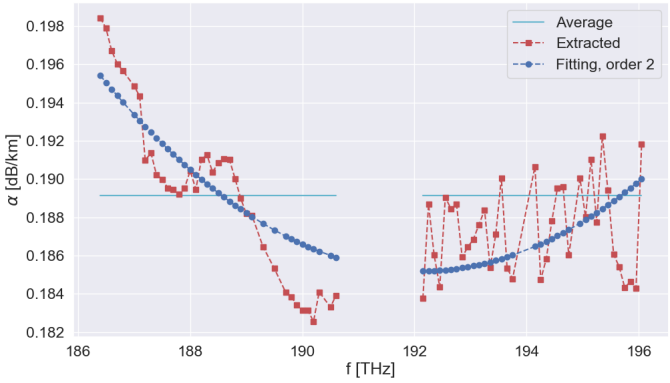


**Fig. 8.** Algorithmic steps for extracting loss coefficient function at channel frequencies $\alpha(f_{ch})$.

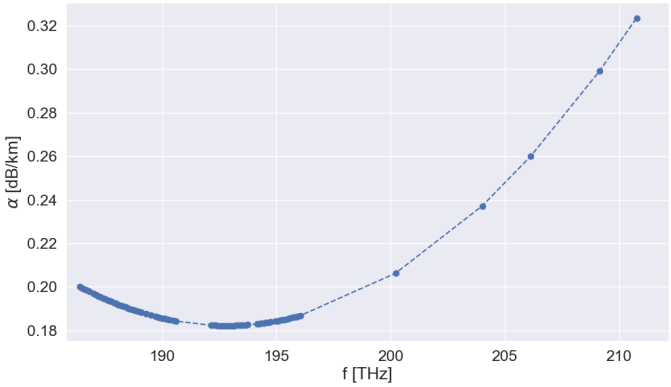


**Fig. 9.** Extracted loss coefficient function.

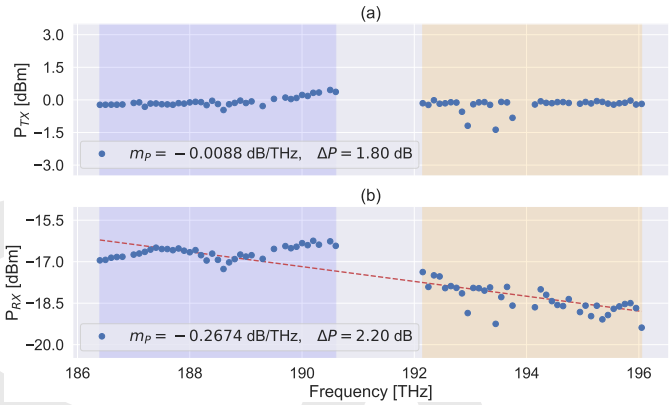


**Fig. 10.** Raman pumps off: (a) transmitted power spectrum, (b) received power spectrum.

C-band (36 channels), and the final WDM spectrum is generated using a C+L coupler. A variable optical attenuator (VOA) have been placed in front of each WDM comb in order to rigidly modify the launch power at the fiber's input. Connecting two standard single mode fiber (SSMF) spools of 60 km and 25 km nominal lengths, a fiber span link of 85 km nominal length is built. At the receiver side, 5 counter-propagating Raman pumps at fixed frequencies spread in [200 - 211] THz frequency range are introduced by means of an optical coupler. In order to emulate telemetry devices, an optical spectrum analyser (OSA) is used at both fiber span terminals. The exchange of information between measurement tools and software modules is not automatized. In this proof-of-concept, we experimentally prove the operation of the conceived system interrogating the OSA to retrieve information regarding the status of the propagating spectrum at the specific node and providing them to the competent software module. On the other hand, the computed Raman pump power configuration is set following embedded laboratory protocols.

### B. Probing Phase Results

Tracing the steps of the proposed probing procedure, the achieved results are reported.

The OTDR analysis carried out on the fiber span link is reported in Tab. 1. Reasonably, there are two insertion losses placed at both fiber span terminals due to the input connector and the output splitter and an intermediate lumped loss due to fiber spools connector.

Following the loss coefficient function at pump frequencies $\alpha(f_p)$, the P&P measurements accurately estimate the strength of the Raman amplification coupling, comparing the extracted value with respect to the theoretical one.

The algorithmic steps for channel loss coefficient function $\alpha(f_{ch})$ are depicted in Fig. 8. This picture clearly expresses the mathematical meaning of Eq. 3: starting from the flat average loss coefficient function $\overline{\alpha}$ (light blue straight line), the frequency content (red square markers) is extracted by exploiting the power difference $\Delta P(f_{ch}, L_S)$ between the real received spectrum and the received one emulated using the average $\overline{\alpha}$. In order to smooth the profile trend, the extracted curve undergoes a polynomial second order fitting (blue circle markers). The result that summarizes the complete extracted loss coefficient function $\alpha(f)$, considering both channels and pumps, is reported in Fig. 9. As last step, the correction parameters are extracted according to Eq. 7 after a system optimization at 10 dB mean gain and flat power spectrum tilt.

| Loss Intensity [dB] | Loss Position [km] |
|---|---|
| 0.2 | 0 |
| 0.2 | 61.0 |
| 0.3 | 86.1 |

**Table 1.** Lumped losses along the fiber span under test.

### C. Measurement Results

After the probing phase, a set of measurements is carried out to verify that the conceived Raman controller architecture works correctly.

Firstly, the WDM spectrum is acquired with Raman pumps turned off (Fig. 10). Having an almost flat input WDM spectrum around 0 dBm per channel, this measurement allows to capture the information regarding the output WDM spectrum tilt $m_P$, useful to emulate amplification constraint on gain tilt. So, by defining the tilt target $m_{G_{OO}}$ to 0.2674 dB/THz, the behaviour of the complete system is tested requiring a gain target $\overline{G_{OO}}$ of 10 dB with a flat output WDM spectrum.

Provided the amplification constraints to the Raman software module, the RDU starts computing the optimal Raman pump power configuration. The optimized Raman pump power config-

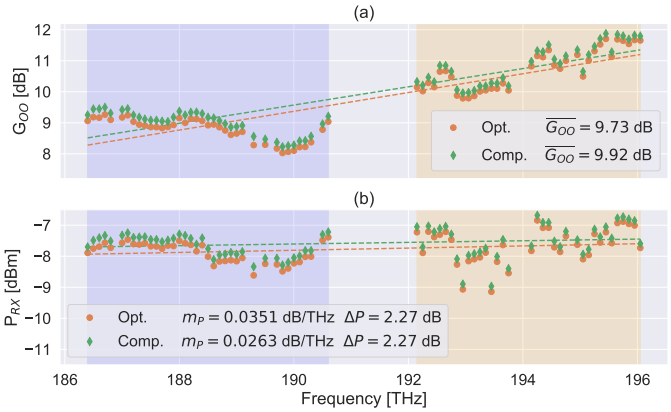


**Fig. 11.** Measured on-off gain profiles with relative metrics.

uration is reported in Tab. 2, where the Raman pump are ordered for decreasing frequency. Subsequently, the RCU sets the Raman pumps as designed by the RDU and it tries to achieve the gain target requested by the control plane within a tolerance of a tenth of dB, linearizing the problem around the optimum working point. The compensated Raman pump power configuration is also reported in Tab. 2.

Fig. 11 displays the effects of the optimized and the compensated configurations in terms of produced on-off gain and output WDM spectrum. The on-off gain $G_{OO}(f)$ is evaluated through the operative definition:

$$G_{OO}(f) = \frac{P_{ON}(f_{ch}, L_S)}{P_{OFF}(f_{ch}, L_S)} \tag{11}$$

where $P_{ON}(f_{ch}, L_S)$ and $P_{OFF}(f_{ch}, L_S)$ are the powers of a specific channel at the end of the fiber span with Raman pumps turned on and off, respectively. The profiles of on-off gain and output WDM spectrum with circular markers is the outcome produced after having set the optimized Raman pump configuration. Thanks to the optimization algorithm, the outcome presents excellent characteristics in terms of tilt and ripple. In fact, the total tilt over the C+L band (about 10 THz) is of some tenths of dB and the maximum deviation with respect to the linear regression of the WDM spectrum undergoes just a small augmentation. As expected, the mean gain is affected by the depletion effect on the Raman pumps due to the channel spectral load, being not able to reach a satisfactory value. On the other hand, the profiles with diamond-fashion markers have been achieved with the Raman pump configuration linearized by the RCU. It is evident that the proposed linearization procedure operates a rigid curve translation that moves the mean gain within the tolerance range without modifying shape and ripple.

| | $P_1$ | $P_2$ | $P_3$ | $P_4$ | $P_5$ |
|---|---|---|---|---|---|
| Frequency [THz] | 210.8 | 209.1 | 206.1 | 204.0 | 200.2 |
| Opt. [mW] | 242.5 | 220.9 | 159.4 | 41.7 | 100.5 |
| Comp. [mW] | 247.1 | 225.1 | 162.4 | 42.5 | 102.4 |

**Table 2.** Raman pump power configurations.

## 7. CONCLUSION

We presented a novel framework for the software abstraction of Raman amplification in multi-band software-defined open and disaggregated optical networks. It is based on a physical layer probing procedure that exploits the telemetry of in-field available OCMs. According to the proposed framework, Raman amplifier sites can be software-abstracted by two modules. Starting from the probed physical layer information, the RDU defines the nominal operational working point designing the optimal Raman pump power configuration according to the gain and tilt targets required by the network controller. The RCU performs the problem linearization around the nominal working point and enables a quick adjustment of the pump levels to counteract changes of operational conditions as spectral and multi-band channel load or physical layer fluctuations. The proposed method has been validated and tested in a lab experiment on a C+L transmission scenario, obtaining excellent results in terms of autonomous Raman amplifier controlling. In particular, within the investigated use case, the implemented methodology achieves the target values of both the mean gain and tilt, producing a minimal distortion of the WDM spectrum as additional ripple never exceeding 0.1 dB.

## ACKNOWLEDGEMENT

The authors would like to thank Alessio Ferrari for his precious support and collaboration.

## REFERENCES

1. J. Bromage, "Raman amplification for fiber communications systems," J. Light. Technol. **22**, 79 (2004).
2. M. N. Islam, "Raman amplifiers for telecommunications," IEEE J. selected topics Quantum Electron. **8**, 548–559 (2002).
3. V. Curri and A. Carena, "Merit of raman pumping in uniform and uncompensated links supporting nywdm transmission," J. Light. Technol. **34**, 554–565 (2015).
4. V. Curri, "System advantages of raman amplifiers," Proc. NFOEC 2000 **1**, 35–46 (2000).
5. W. S. Pelouch, "Raman amplification: An enabling technology for long-haul coherent transmission systems," J. Light. Technol. **34**, 6–19 (2015).
6. M. Tan, P. Rosa, S. T. Le, I. D. Phillips, and P. Harper, "Evaluation of 100g dp-qpsk long-haul transmission performance using second order co-pumped raman laser based amplification," Opt. express **23**, 22181–22189 (2015).
7. V. E. Perlin and H. G. Winful, "On distributed raman amplification for ultrabroad-band long-haul wdm systems," J. lightwave technology **20**, 409 (2002).
8. S. Namiki and Y. Emori, "Ultrabroad-band raman amplifiers pumped and gain-equalized by wavelength-division-multiplexed high-power laser diodes," IEEE J. Sel. Top. Quantum Electron. **7**, 3–16 (2001).
9. A. Carena, V. Curri, and P. Poggiolini, "On the optimization of hybrid raman/erbium-doped fiber amplifiers," IEEE Photonics Technol. Lett. **13**, 1170–1172 (2001).
10. T. J. Xia, H. Fevrier, T. Wang, and T. Morioka, "Introduction of spectrally and spatially flexible optical networks," IEEE Commun. Mag. **53**, 24–33 (2015).
11. G. S. Zervas and D. Simeonidou, "Cognitive optical networks: Need, requirements and architecture," in *2010 12th International Conference on Transparent Optical Networks,* (IEEE, 2010), pp. 1–4.
12. B. Correia, R. Sadeghi, E. Virgillito, A. Napoli, N. Costa, J. Pedro, and V. Curri, "Networking performance of power optimized c+l+s multiband transmission," in *GLOBECOM 2020 - 2020 IEEE Global Communications Conference,* (2020), pp. 1–6.

13. M.-S. Kao and J. Wu, "Signal light amplification by stimulated raman scattering in an n-channel wdm optical fiber communication system," J. lightwave Technol. **7**, 1290–1299 (1989).
14. Y. Emori, K. Tanaka, and S. Namiki, "100 nm bandwidth flat-gain raman amplifiers pumped and gain-equalised by 12-wavelength-channel wdm laser diode unit," Electron. Lett. **35**, 1355–1356 (1999).
15. V. E. Perlin and H. G. Winful, "Optimal design of flat-gain wide-band fiber raman amplifiers," J. lightwave technology **20**, 250 (2002).
16. X. Liu and Y. Li, "Optimizing the bandwidth and noise performance of distributed multi-pump raman amplifiers," Opt. communications **230**, 425–431 (2004).
17. B. Neto, A. J. Teixeira, N. Wada, and P. André, "Efficient use of hybrid genetic algorithms in the gain optimization of distributed raman amplifiers," Opt. express **15**, 17520–17528 (2007).
18. X. Zhao, V. Vusirikala, B. Koley, V. Kamalov, and T. Hofmeister, "The prospect of inter-data-center optical networks," IEEE Commun. Mag. **51**, 32–38 (2013).
19. X. Zhao, V. Vusirikala, B. Koley, T. Hofmeister, V. Kamalov, and V. Dangui, "Optical transport sdn for high-capacity inter-datacenter networks," in *Photonics in Switching,* (Optical Society of America, 2014), pp. PM3C–1.
20. A. Caballero, R. Borkowski, D. Zibar, and I. T. Monroy, "Performance monitoring techniques supporting cognitive optical networking," in *2013 15th International Conference on Transparent Optical Networks (ICTON),* (IEEE, 2013), pp. 1–4.
21. R. Borkowski, R. J. Duran, C. Kachris, D. Siracusa, A. Caballero, N. Fernandez, D. Klonidis, A. Francescon, T. Jimenez, J. C. Aguado *et al.*, "Cognitive optical network testbed: Eu project chron," J. Opt. Commun. Netw. **7**, A344–A355 (2015).
22. D. Zibar, A. Ferrari, V. Curri, and A. Carena, "Machine learning-based raman amplifier design," in *Optical Fiber Communication Conference,* (Optical Society of America, 2019), pp. M1J–1.
23. D. Zibar, A. M. R. Brusin, U. C. Moura, V. Curri, and A. Carena, "Inverse system design using machine learning: the raman amplifier case," J. Light. Technol. (2019).
24. A. M. R. Brusin, U. C. De Moura, A. D'Amico, V. Curri, D. Zibar, and A. Carena, "Load aware raman gain profile prediction in dynamic multi-band optical networks," in *2020 Optical Fiber Communications Conference and Exhibition (OFC),* (IEEE, 2020), pp. 1–3.
25. G. Borraccini, A. Ferrari, S. Straullu, A. Nespola, A. D'Amico, S. Piciaccia, G. Galimberti, A. Tanzi, S. Turolla, and V. Curri, "Softwarized and autonomous raman amplifiers in multi-band open optical networks," in *International IFIP Conference on Optical Network Design and Modeling,* (2020).
26. G. Borraccini, S. Straullu, A. Ferrari, S. Piciaccia, G. Galimberti, and V. Curri, "Flexible and autonomous multi-band raman amplifiers," in *2020 IEEE Photonics Conference (IPC),* (IEEE, 2020), pp. 1–2.
27. G. Borraccini, S. Staullu, A. Ferrari, S. Piciaccia, G. Galimberti, A. Tanzi, and V. Curri, "Autonomous raman amplifiers in software-defined optical transport networks," in *GLOBECOM 2020 - 2020 IEEE Global Communications Conference,* (2020), pp. 1–6.
28. G. Borraccini, S. Staullu, S. Piciaccia, A. Tanzi, A. Nespola, G. Galimberti, and V. Curri, "Autonomous raman amplifiers using standard integrated network equipment," IEEE Photonics Technol. Lett. (Early Access Article) (2021).
29. S. Gringeri, B. Basch, V. Shukla, R. Egorov, and T. J. Xia, "Flexible architectures for optical transport nodes and networks," IEEE Commun. Mag. **48**, 40–50 (2010).
30. E. Riccardi, P. Gunning, Ó. G. de Dios, M. Quagliotti, V. López, and A. Lord, "An operator view on the introduction of white boxes into optical networks," J. Light. Technol. **36**, 3062–3072 (2018).
31. J. Kundrát, O. Havliš, J. Jedlinskỳ, and J. Vojtěch, "Opening up roadms: Let us build a disaggregated open optical line system," J. Light. Technol. **37**, 4041–4051 (2019).
32. M. Birk, O. Renais, G. Lambert, C. Betoule, G. Thouenon, A. Triki, D. Bhardwaj, S. Vachhani, N. Padi, and S. Tse, "The openroadm initiative," IEEE/OSA J. Opt. Commun. Netw. **12**, C58–C67 (2020).
33. C. Manso, R. Muñoz, N. Yoshikane, R. Casellas, R. Vilalta, R. Martínez, T. Tsuritani, and I. Morita, "Tapi-enabled sdn control for partially disaggregated multi-domain (ols) and multi-layer (wdm over sdm) optical networks," J. Opt. Commun. Netw. **13**, A21–A33 (2021).
34. J. Bromage, K. Rottwitt, and M. Lines, "A method to predict the raman gain spectra of germanosilicate fibers with arbitrary index profiles," IEEE Photonics Technol. Lett. **14**, 24–26 (2002).
35. E. Pincemin, D. Grot, L. Bathany, S. Gosselin, M. Joindot, S. Bordais, Y. Jaouen, and J.-M. Delavaux, "Raman gain efficiencies of modern terrestrial transmission fibers in s-, c-and l-band," in *Nonlinear Guided Waves and Their Applications,* (Optical Society of America, 2002), p. NLTuC2.